Physica D 62 (1993) 263–274
North-Holland

PHYSICA D

Genesis of bursting oscillations in the Hindmarsh–Rose model and homoclinicity to a chaotic saddle

X.-J. Wang

Mathematical Research Branch, NIDDK, National Institutes of Health, Bethesda, MD 20892, USA and Department of Mathematics and the James Franck Institute, University of Chicago, 5734 S. University Av., Chicago, IL 60637, USA[1]

We present two hypotheses on the mathematical mechanism underlying bursting dynamics in a class of differential systems: (1) that the transition from continuous firing of spikes to bursting is caused by a crisis which destabilizes a chaotic state of continuous spiking; and (2) that the bursting corresponds to a homoclinicity to this unstable chaotic state. These propositions are supported by a numerical test on the Hindmarsh–Rose model, a prototype of its kind. We conclude by a unified view for three types of complex multi-modal oscillations: homoclinic systems, bursting, and the Pomeau–Manneville intermittency.

1. Introduction

1.1. Prelude

By *bursting oscillation* we mean here a time evolution consisting of bursts of rapid spikes, alternated by phases of relative quiescence. It is often in this form of membrane electrical activity that cells in the biological nervous system are involved in various rhythmic behaviours, such as central pattern generations in invertebrates [24], or pacemakers of brain waves in the mammalian cortex [27]. It is therefore a question of biological interest to ask how a rhythm (of bursting) can come about, starting from the "building blocks" of the neuronal electrical activity, the action potentials. An individual cell capable of bursting may be at rest or merely exhibit continuous firing of action potentials, when it is subject to different electrical stimuli. Spikes within bursts in a bursting state and those in a continuous spiking state are generated by the same ionic currents. This obvious biophysical fact provides a main ingredient to theoretical models of bursting in excitable cells, where bursting oscillations are viewed as switching back and forth between a continuous spiking state and a quiescent (resting) state [11,19,20].

In this paper we seek to express this picture of bursting in a precise mathematical form. For definiteness, we shall consider a deterministic model due to Hindmarsh and Rose (HR) [11]. The HR model shares essential qualitative features with several other biophysical models of excitable cells, such as the Chay–Keizer equations for the insulin-secreting β-cells of the pancreas [2], the generalized Morris–Lecar equations for the barnacle muscle fiber [14,22], or the Decroly–Goldbeter equations for enzyme reactions [4]. But it is simpler, consisting of three differential equations with only quadratic and cubic algebraic nonlinearities. For this class of systems, we would like to suggest that the transition from a continuous spiking state to a bursting state occurs when the former becomes chaotic, and this chaotic state is in turn destabilized. Moreover, we propose that the genesis of the bursting state corresponds to the realization of a homoclinic mechanism to this unstable chaotic state.

[1] Present address.

0167-2789/93/$06.00

1.2. Homoclinicity to a chaotic saddle

In a three-dimensional dissipative system, the Lyapunov exponents of a chaotic state Ω must be of the type $(+, 0, -)$, i.e., $\lambda_u > \lambda_0 = 0 > \lambda_s$, with $|\lambda_s| > \lambda_u$. The positive exponent λ_u characterizes the sensitivity to initial conditions, and a Kolmogorov–Sinai entropy h_{KS} quantifies the randomness of the dynamics. According to a Ruelle inequality [6], we have $\lambda_u \geq h_{KS}$. The equality holds if Ω is asymptotically stable. Otherwise, it is nonattracting, and trajectories in a neighborhood of Ω would escape from it with a mean rate of $\gamma = \lambda_u - h_{KS} > 0$. The attractiveness of Ω may be expressed in an alternative way: it is stable if it includes its own unstable manifold $W_u(\Omega)$; when Ω becomes unstable, $W_u(\Omega)$ will no longer be confined in Ω, and can emanate to other regions of the phase space.

We shall define a homoclinicity to a chaotic saddle Ω by the following conditions: (1) Ω is chaotic ($h_{KS} > 0$) and nonattracting ($\gamma > 0$); (2) Ω is endowed with a hyperbolic structure (cf. [6] for a definition), in which case Ω is called a saddle; and (3) there exists a reinjection mechanism, by which the outgoing unstable manifold $W_u(\Omega)$ of Ω is brought back to the vicinity of this same state, along its stable direction, and intersects with its stable manifold $W_s(\Omega)$. Such a situation is illustrated in fig. 1.

Homoclinicity to a chaotic set [8,15] presents another class of homoclinic systems to an invariant set Ω of saddle nature; be it a Šil'nikov saddle–focus equilibrium point [25], a periodic cycle [9], or a quasiperiodic torus [26]. Homoclinic mechanisms have proved to be relevant to a wide variety of nonlinear systems which display mixed-mode oscillations, with the two disparate time scales related to the subdynamics near Ω and to the reinjection loop, respectively.

Homoclinic systems are particularly interesting near the situation of a tangency, when $W_s(\Omega)$ is tangent to $W_u(\Omega)$. In this way a system becomes structurally unstable, and complex bifurcation phenomena appear. In the case of homoclinic tangency to a basic cycle, Newhouse [16,23] proved the following: near the tangency, a hyperbolic chaotic set of orbits is created, to which *secondary* homoclinicities are realized and *persist* for an open set of parameter values. As a con-

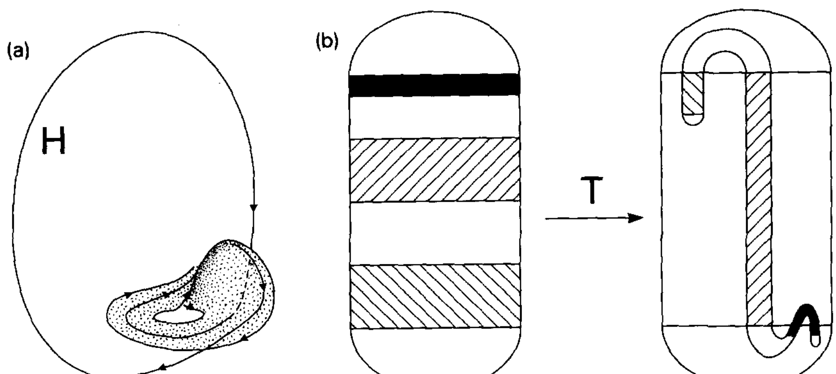

Fig. 1. (a) Illustration of homoclinicity to a chaotic saddle. The chaotic invariant set is not stable. Due to a reinjection mechanism, its outgoing unstable manifold is brought back to the vicinity of the set, and intersect with the stable manifold. (b) Poincaré section of a homoclinic system to a variant of the Smale horseshoe. The map T has a unique fixed point, and possesses a chaotic invariant set Ω. The local stable (resp. unstable) manifold of Ω forms a Cantor family of horizontal (resp. vertical) straight lines. The reinjection is shown by the image of the black horizontal strip by one iteration of T. In concrete model systems several iterations may be needed to bring the orbits escaping from Ω back to its neighborhood again. This picture suggests a decomposition of the map T into two subsystems: the local map T_0 which is defined in a neighborhood of Ω; and the global map T_1 which describes the reinjection.

sequence, there is a parameter set (the Newhouse set), for which infinitely many periodic *attractors* of arbitrarily long period coexist in a bounded region of the phase space. The same conclusion has been obtained more recently in the case of a Šil'nikov saddle–focus fixed point [17]. In this sense, homoclinicity to a chaotic saddle is of relevance also to these two other situations. In particular, it has been used to investigate the Newhouse phenomenon, and the Newhouse parameter set was proved to possess a strictly positive Hausdorff dimension in the parameter space [32]. The question of whether the Newhouse set has a positive Lebesgue measure remains open [28,32].

1.3. *Crisis of a chaotic state*

We shall construct numerically a chaotic saddle of continuous spiking in the bursting regime of the HR model. Recently, Terman proved analytically that in a range of parameter values in the bursting regime, there exists a hyperbolic set of orbits which corresponds to spikes and is not attracting [30]. Although the hyperbolic chaotic set we identified is not the same as Terman's, this author's work was a source of inspiration. Furthermore, we shall provide evidence that a homoclinic mechanism is realized to the unstable continuous spiking chaos, which underlies the bursting dynamics. On the basis of Terman's approach we believe that the existence of homoclinic orbits can be confirmed by a rigorous analysis.

On the other hand, we know that Ω *is* attracting in another range of parameter values, where the system displays continuous spiking. The interesting question arises, therefore, as to the nature of the transition from one regime to the other. We shall show that Ω loses its stability when it merges with an invariant manifold of an unstable equilibrium point. Thus the transition may be viewed as a *crisis* [10] for Ω. The order parameter of this transition is the mean escape rate γ, which is zero in the continuous spiking regime, and positive in the bursting regime. By adopting an argument from [10], a power law is predicted, according to which γ tends to zero as the criticality is approached from the bursting side. The exponent α of this power law has been estimated numerically and agrees with the theoretical value, $\alpha = 1/2$.

Finally we conclude by pointing out a similarity between the bursting dynamics near the crisis, and the Pomeau–Manneville intermittent dynamics. Thus, both these dynamics, as well as the homoclinic systems of various types, can all be included in a single framework of mathematical description.

2. The Hindmarsh–Rose model

2.1. *Dynamics and bifurcations*

The system under study is [11]

$$\mathrm{d}x/\mathrm{d}t = y - x^3 + 3x^2 - z\,, \tag{1}$$

$$\mathrm{d}y/\mathrm{d}t = 1 - 5x^2 - y\,, \tag{2}$$

$$\mathrm{d}z/\mathrm{d}t = \epsilon[x - (z - z_0)/4]\,, \tag{3}$$

which depends on two parameters z_0 and ϵ. The variable x represents the membrane potential, y a recovery variable, and z an adaptation variable which changes slowly ($\epsilon \ll 1$). Note that a constant current applied to x can be absorbed into z_0 by a simple redefinition of z.

In what follows we shall fix $\epsilon = 0.004$, and discuss the dynamics of the HR system as z_0 is varied. As z_0 is increased, four dynamic regions have been found (cf. also [12], and [3] for the Chay–Keizer model). They are summarized briefly as follows:

Region IV. An equilibrium state with moderate x level. It is a stable focus for $z_0 < (z_0)_{\text{III–IV}} \simeq -18.86$, where it loses its stability via a Hopf bifurcation.

Region III. A limit cycle of continuous spiking arises at $(z_0)_{\text{III-IV}}$. It covers a wide range of z_0 and becomes unstable by a period doubling at $z_0 \simeq 3.11$. As z_0 is further increased, a period doubling cascade [7] takes place, leading to *chaotic* firing of spikes. Next, a transition occurs, where bursting starts to substitute for continuous spiking. THe nature of this transition will be a focus of discussion in what follows.

Region II. So, above the critical value

$$(z_0)_{\text{II-III}} = 3.15867947 \pm 10^{-8} \tag{4}$$

bursting oscillations occur. The bursting state is chaotic for z_0 values immediately above the criticality. However, there exist also a few small periodic windows in this range of z_0. For $z_0 > 3.2$, no chaos has been seen. Instead, a regular sequence of periodic bursting attractors was found. This sequence ends at $(z_0)_{\text{I-II}} \simeq 5.13$.

Region I. For $z_0 > (z_0)_{\text{I-II}}$, the attractor is an equilibrium node at low x level.

We shall mainly be concerned with the rhythmogenesis of bursting dynamics in region II, near the border with region III.

2.2. Periodic and chaotic bursting

As illustrated in fig. 2a, a periodic bursting oscillation consists of regular alternations between bursts of spikes and phases of near steady state quiescence. Following Rinzel [19], a rather suggestive picture of bursting emerges, when we project this orbit onto the xz-plane, and

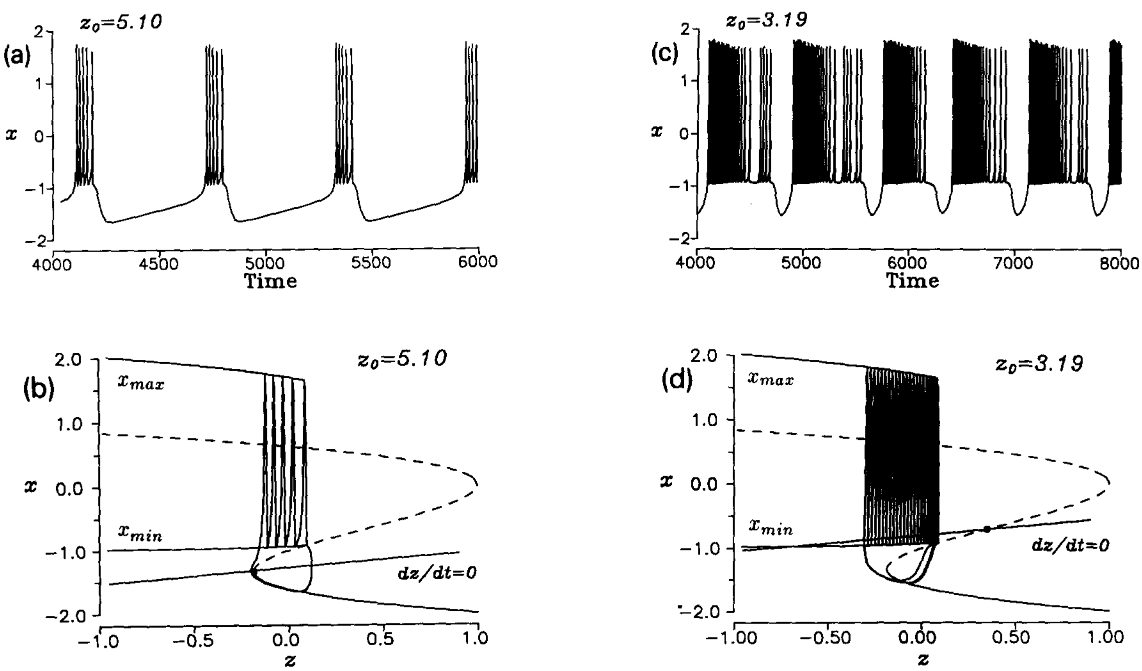

Fig. 2. Periodic (a), (b) and chaotic bursting (c), (d). In (b) and (d), the bursting orbits are projected on the xz-plane. Superimposed is the bifurcation diagram of the fast subsystem, with a Z-shaped steady state curve (solid: stable; dashed: unstable) and a branch of periodic solutions indicated by the minimum and maximum of the x-component. For (a) and (c), eqs. (1)–(3) were integrated by using a subroutine called LSODE (standing for the Livermore Solver for Ordinary Differential Equations, 1981 Version). A Gear method was used to handle the stiffness of the system. The same initial condition was used thoroughly: $x = -1.1804$, $y = -5.809943$ and $z = 0.02212644$.

superimpose it with the bifurcation diagram for the fast xy subsystem (fig. 2b). The xy system, with $\epsilon = 0$ and with its control parameter $z =$ const., has a Z-shaped steady state curve and a branch of periodic solutions which terminates at a homoclinic point $z = z_c$. In a bursting oscillation of the full system, the z variation is confined approximatively between the lower knee of the steady state Z-curve and the homoclinic point z_c of the xy system (fig. 2b). In this range of z there is a bistability in the xy system, with a stable steady state and a limit cycle. On the other hand, the z-nullcline, $x = (z - z_0)/4$, divides the xz-plane into two parts: above the nullcline $dz/dt > 0$ and z slowly increases, whereas the opposite is true below the nullcline. Consequently if the z-nullcline lies somewhere in the middle of the two regions of coexisting attractors in the xy system, an orbit can undergo several spikes as z is increased above the z-nullcline until it reaches z_c, when the orbit drops down to the lower steady state branch of the xy system. Then z starts to decrease as x slowly drifts up to the knee of that branch, when the orbit is reinjected to the upper oscillatory region, and the process restarts itself ab initio.

A unique equilibrium state p of the complete system is determined by the intersection of the z-nullcline and the steady state Z-curve of the fast subsystem. In the bursting regime the z-nullcline intersects with the middle branch of the Z-curve, hence p is a saddle. Let us denote its three linear stability eigenvalues as $\lambda_s < 0 < \lambda_u' < \lambda_u$, and the corresponding invariant manifolds as $W_s(p)$, $W_u'(p)$ and $W_u(p)$, respectively. We know that λ_u' is vanishingly small as $\epsilon \to 0$, and is relatively unimportant for the local behavior around p. Then, if an oscillatory orbit approaches the equilibrium state, it faces a situation similar to that of the homoclinic loop of the xy system. Its period is lengthened (cf. fig. 2a), and bypassing the equilibrium state p it eventually escapes from it along one of the two eigendirections of $W_u(p)$. Now, along one eigendirection the x-component is increasing, thus the orbit will remain in the oscillatory region; whereas along the other eigendirection the x-component is *decreasing*, so that the orbit is sent to the lower steady state branch of the xy system.

The decisive role for p, as suggested above, is especially evident if p is close to the homoclinic point of the xy system, where bursts invariably terminate (cf. fig. 2a). In other words, the z-component z^* of p must be close to z_c. This is expected to be the case near the transition from continuous spiking to bursting, since as $\epsilon \to 0$ the value of $(z_0)_{\text{II-III}}$ is determined by the condition $z^*(z_0) = z_c$. Numerically, however, the value of $(z_0)_{\text{II-III}}$ is usually found to be lower than that predicted by this condition, even for seemingly small values of ϵ (e.g. eq. (4) compared with the predicted value $z_0 \simeq 3.77$ for $\epsilon = 0.004$. See also [21]). In fig. 2c, d is shown an example of chaotic bursting at $z_0 = 3.19$, where z^* is significantly above z_c. We also tested $\epsilon = 0.0005$ and 0.0001, in addition to 0.004, which led to the same conclusion.

Nevertheless, one may slightly generalize the above reasoning with a weaker assumption about how close an oscillatory orbit must come to the equilibrium state p. In fact, the above reasoning can be repeated, with the role of p replaced by that of the unstable manifold $W_u'(p)$. Thus, the two-dimensional manifold $W_s(p) \times W_u'(p)$ would separate the two eigendirections of $W_u(p)$, and as an orbit approaches $W_s(p) \times W_u'(p)$, it would either stay in the oscillatory region or escape from it, depending on which side of this 2D surface it would fall. Expressed in this way, we may surmise the following *transition criterion*: an attractor of continuous spiking is restricted to one side of the invariant manifold $W_s(p) \times W_u'(p)$ of the equilibrium state p, while a transition to bursting occurs when orbits are allowed to escape to the other side.

2.3. *Test of the transition criterion*

We construct a Poincaré section, which is defined by the intersection of the flow with a surface in the phase space. We chose this surface as a plane Π very close to the equilibrium state p,

$$\Pi: x = x^* + 10^{-5}, \tag{5}$$

where x^* is the x-component of p. The sense of intersection was fixed to be from above to below the plane.

A Poincaré section is obtained numerically from the intersection of a long orbit with the plane Π. Also computed is the *linearized* $W_s(p) \times W_u'(p)$, and its intersection with the plane Π. This straight line segment, say $y = w(z; z_0)$, is an approximation of the one-dimensional curve $W_s(p) \times W_u'(p) \cap \Pi$. In principle, if ϵ is not infinitesimally small, so that the equilibrium state p is not close to the homoclinic point near $z_0 = (z_0)_{\mathrm{II-III}}$, the *global* (nonlinear) invariant manifolds would have been needed. We used the linear approximation instead, merely because of our inability to construct the global $W_s(p) \times W_u'(p)$ numerically. In terms of the Poincaré section, the *transition criterion* asserts that an attractor of continuous spiking is confined to one side of the linear segment $y = w(z; z_0)$, and the transition to bursting occurs when orbits are allowed to escape to the other side. This criterion was found numerically to be consistent with other ways to distinguish a bursting regime from a continuous firing one, such as visual inspection of time traces. Indeed, applying this criterion we were able to locate the critical point $(z_0)_{\mathrm{II-III}}$ of the transition, eq. (4), with high accuracy (see figs. 3a, b). Fig. 3 presents convincing evidence in favor of the posited *transition criterion*.

The attractors in the Poincaré section of fig. 3 are compressed approximatively onto a one-dimensional (1D) curve in the plane, near the unstable manifold of the fixed point of the Poincaré map (the basic continuous spiking cycle). This remarkable feature has also been found in other biophysical models of bursting [1], and is a consequence of strong contraction transversal to the attractor. For instance, the stable eigenvalue Λ_s of the basic cycle was found to be $|\Lambda_s| < 10^{-12}$ for the z_0 values of fig. 3. Let this 1D curve be denoted by $y = \tilde{y}(z; z_0)$. The invariant manifold $W_s(p) \times W_u'(p) \cap \Pi$ divides this 1D curve into two parts, with the middle point $z = z_b$ determined by $w(z_b; z_0) = \tilde{y}(z_b; z_0)$ (cf. fig. 4a).

Moreover, the two-dimensional Poincaré map

$$T: \begin{cases} z_{n+1} = F(y_n, z_n; z_0), \\ y_{n+1} = G(y_n, z_n; z_0) \end{cases} \tag{6}$$

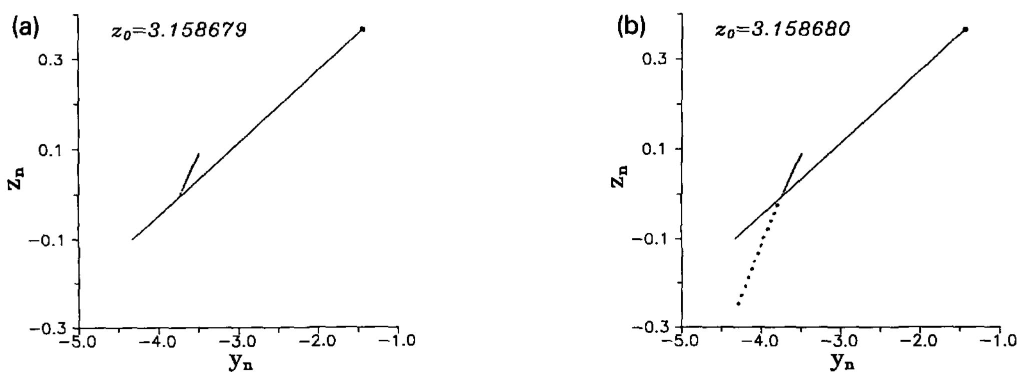

Fig. 3. Poincaré section of attractors on a plane Π, for two very close values of z_0 below (a) and above (b) the continuous spiking–bursting transition. The solid circle at the upper right is the intersection with the plane of the stable manifold $W_s(p)$ of the equilibrium state p of the system. The straight solid line $y = w(z; z_0)$ is the intersection with the plane of the linearized invariant manifold $W_s(p) \times W_u'(p)$. This figure demonstrates that the continuous spiking state is confined to one (the upper) side of $y = w(z; z_0)$, and bursting occurs when this state is enlarged to merge with $y = w(z; z_0)$.

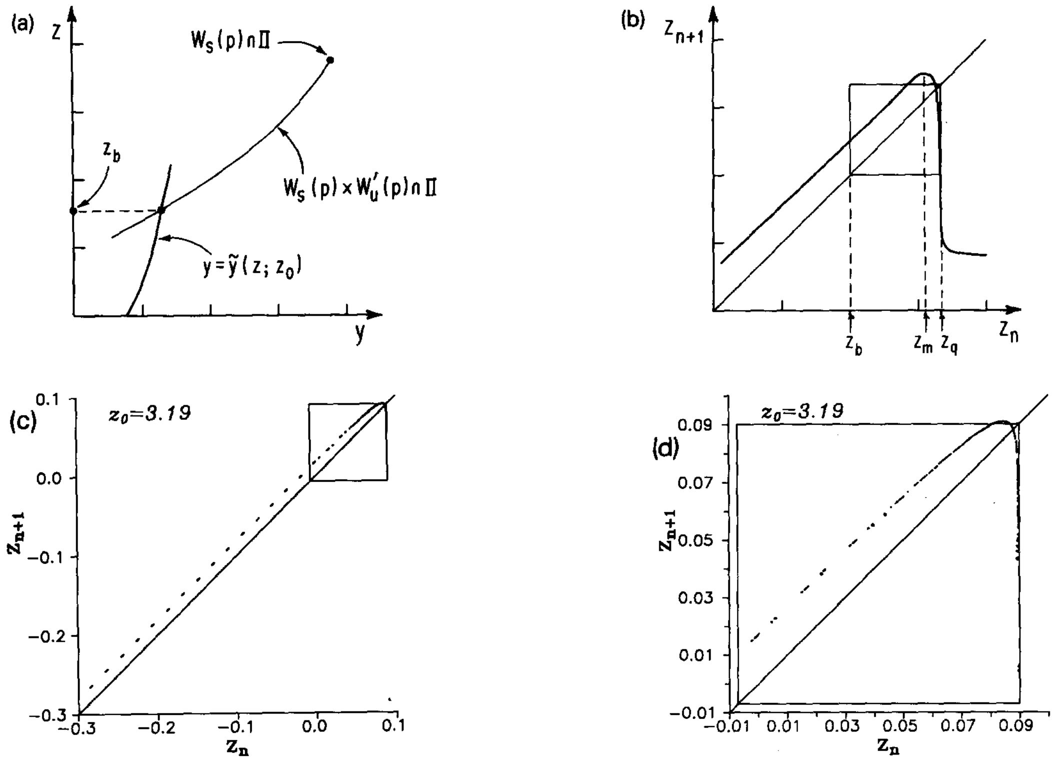

Fig. 4. (a) Schematic illustration of the Poincaré section. The attractor is collapsed onto a 1D curve $y = \tilde{y}(z; z_0)$. The point at $z = z_b$ is the intersection of this curve with the invariant manifold $W_s(p) \times W_u'(p) \cap \Pi$. (b) The reduced 1D map $z_{n+1} = f(z_n; z_0)$. The point z_q is one of the two preimages of z_b, and z_m is the location of the maximum of the map. (c) The 1D map for $z_0 = 3.19$. The square window delimits the definition domain of the continuous spiking subdynamics, $\Delta = [z_b, z_q]$. (d) An enlarged view of the local map T_0. The chaotic invariant set of T_0 is not attracting, because the maximum of the map exceeds the definition domain. This is in contrast with the continuous spiking case (not shown).

is reduced to a 1D map

$$z_{n+1} = F(\tilde{y}(z_n; z_0), z_n; z_0) \equiv f(z_n; z_0) , \qquad (7)$$

as is schematically shown in fig. 4b.

The function $f(z; z_0)$ possesses a unique maximum, say at $z = z_m$. We define f_A on $z < z_m$ as the part of f that is strictly increasing, and f_B on $z > z_m$ as the part of f that is strictly decreasing. Let $z_q = f_B^{-1}(z_b)$. Then, in terms of the 1D map, the *transition criterion* is expressed as follows: a continuous spiking state is confined in the interval $[z_b, z_q]$, and bursting occurs when orbits are allowed to escape from this interval.

The 1D attractor corresponding to a chaotic bursting regime at $z_0 = 3.19$ is displayed in fig. 4c. The portion on $[z_b, z_q]$ is marked by a square window, and enlarged in fig. 4d. Note that the map $z_{n+1} = f(z_n; z_0 = 3.19)$ may be obtained by a method used in [3], which would yield a form similar to fig. 4b.

2.4. Hyperbolic chaos and reinjection

Suppose that we are in the bursting region II. We denote by T_0 the 1D map restricted to the interval $\Delta = [z_b, z_q]$, the definition domain of the continuous spiking subdynamics. T_0 is of logistic type, and has a single fixed point.

The maximum of T_0 at z_m exceeds the definition domain Δ, $f(z_m) > z_q$, so that orbits may fall into $[f_A^{-1}(z_q), f_B^{-1}(z_q)]$, and escape from Δ. Let $\Delta' = f[f_A^{-1}(z_q), \;\; f_B^{-1}(z_q)] = [z_q, f(z_m)]$. The image of Δ' by f is a very small interval located on the left side of Δ, where f has a slope near to unity. Due to the channel-like form of f, by further iterations Δ' is simply moved upwards without deformation, and must eventually enter the interval Δ. (At $z_0 = 3.19$, for instance, the required number of iterations is $k = 16$, given by the number of dots seen outside Δ in fig. 4c.) Thus, there exists an integer k, such that f^k projects the interval Δ' back to Δ. We shall denote by T_1 the reinjection map f^k restricted on Δ'.

Note that the integer k depends sensitively on ϵ, because of the channel-like form of the f-function for $z < z_b$. For smaller ϵ, the channel is tighter, covers a narrower range of z, and eventually shrinks to a point of the diagonal straight line. This reflects the fact that as ϵ tends to 0, both the speed and the range of the z variation vanish, and continuous spiking can last indefinitely.

In terms of the two subdynamics T_0 and T_1, with their aforementioned properties, we can show that all three conditions for a realization of homoclinicity to a chaotic saddle can be fulfilled:

(1) the invariant set Ω of T_0 is chaotic, and nonattracting. The chaotic nature of Ω can be proved by applying a theorem of Li and Yorke [13]. The proof is strictly similar to that carried out in [8], which we shall not reiterate. Recall that the Li–Yorke theorem implies that there exists an invariant set of orbits included in Ω which is not countable and forms a Cantor set.

That Ω is not attracting in region II follows immediately from the fact that the maximum of T_0 exceeds the definition domain Δ of T_0. This is true for z_0 in the bursting region II, not in the continuous spiking region III.

(2) the invariant set Ω is endowed with a hyperbolic structure. It can be shown that $|T_0'|^{-1/2}$ is a convex function, so that the Schwartzian derivative of T_0 is negative for $z \in \Delta$. This combined with the fact that $T_0(z_m) > z_q$ is sufficient (cf. [31]) to imply a hyperbolic structure for Ω, in the sense that there exist a $K > 0$ and $\theta > 1$, such that $|(T_0^n)'(z)| > K\theta^n$, for all $n \geq 1$ and for all $z \in \Omega$. The invariant state of continuous spiking Ω is thus a chaotic saddle.

(3) a reinjection mechanism is realized by T_1, since $T_1(\Delta') \subset \Delta$. For parameter z_0 values such that $T_1(\Delta')$ is not in any gap of the Cantor set Ω, $T_1(\Delta') \cap \Omega \neq \emptyset$. Thus, there are points in Δ' which converge to Ω after k iterations of f. These correspond to homoclinic orbits since their iterates by f^{-n} also tend asymptotically to Ω.

In conclusion, a bursting dynamics can be expressed as a reinjection mechanism to a chaotic saddle of continuous spiking. Its Poincaré map is similar to that sketched in fig. 1b, with two differences: the transversal compression is very strong, so that the map is reduced to an one-dimensional one; and the reinjection consists of a number of iterations which can be larger for small ϵ values. Hence, bursting dynamics is distinguished from other homoclinic systems, in that its global reinjection map may be rather subtle.

2.5. Complex sequences of bursting cycles

The destabilization of the continuous spiking chaotic state Ω and a homoclinic mechanism to it not only generate an enlarged chaotic state (of bursting oscillations), but also lead to the creation of a plethora of *periodic attractors*. This is because the invariant set Ω contains a countable infinity of periodic orbits, all of the saddle type; and a homoclinic tangency to each of these cycles can create an infinite sequence of periodic windows in the parameter space. For instance, suppose that a homoclinic tangency to the fixed point of the Poincaré map is realized at z_0^*. Then, periodic bursting with n spikes per period bifurcate at $(z_0)_n^t$ which accumulate at z_0^*, and they remain stable for parameter ranges $(\Delta z_0)_n$ which tend to zero as $n \to \infty$. We have [8,9,23]

$$(z_0)_n^t - z_0^* \sim \text{const.} \times \Lambda_u^{-n} ,$$

$$(\Delta z_0)_n \sim \text{const.} \times \Lambda_u^{-2n} , \qquad (8)$$

where Λ_u is the unstable eigenvalue of the fixed point. Thus, periodic windows near a homoclinic tangency typically converge according to an exponential law, with the rate given by Λ_u. Furthermore, in contrast to the case with $\Lambda_u > 0$, where the whole sequence shows a simple order, if $\Lambda_u < 0$, there is a subsequence of which the even values of n are located on one side of z_0^*, while the odd ones are on the other side.

Since the periodic window width in such a sequence vanishes exponentially, as $n \to \infty$, a numerical observation of eq. (8) is feasible only if $|\Lambda_u|$ is not too large. In the case of the HR model, we used the AUTO program [5] to estimate Λ_u as function of z_0. At the period doubling point $z_0 \simeq 3.11$, $\Lambda_u = -1$. As z_0 is further increased, $|\Lambda_u|$ was found to increase sharply, and become more negative than -100 for $z_0 > 3.45$. This implies that such a bifurcation sequence can be relevant at most for a small range of z_0 in the bursting region II. On the other hand, close to the transition point $(z_0)_{\text{II-III}} = 3.15867947 \pm 10^{-8}$, we observed numerically two consecutive periodic windows: $n = 23$ for $z_0 \in [3.168, 3.18]$ and $n = 25$ for $z_0 \in [3.16, 3.161]$, with no discernable $n = 24$ window between the two. Chaos was found for $z_0 \in [3.162, 3.167]$. Hence, perhaps a homoclinic tangency is realized to the fixed point of the Poincaré map at z_0 near 3.16.

Similar consideration can be carried out for periodic orbits of higher order, but the related periodic windows would be even narrower in the parameter space. To classify all the possible periodic windows generated by homoclinic tangencies, one needs a symbolic dynamics description. Let us partition the interval Δ into two domains,

$$\Delta_0 = \{z \colon z_b < z < f_B^{-1}(z_m)\}\,, \tag{9}$$

$$\Delta_1 = \{z \colon f_B^{-1}(z_m) < z < z_q\}\,. \tag{10}$$

This particular choice, which is analogous to that used in [8], is made so that (1) only in Δ_1 is the return time sharply increased; (2) the unique fixed point belongs to Δ_0; (3) the quiescent phase is always preceded by a spike of type 0; and (4) a spike of type 1 is always followed by a spike of type 0. This last condition is in keeping with the numerical observation that a spike with conspicuously large return time is always followed by a spike with a short return time (see fig. 2c for an example).

Furthermore, one iteration by f from a point in Δ' corresponds to a spike followed by a silent phase, which we denote by the symbol 0S. Then, the symbol assigned to one iteration by T_1 should be $0S0^{k-1}$. Equipped with this symbolic dynamics of spiking and reinjection, all the periodic windows can be classified according to their symbolic names. For instance, the aforementioned two windows with $n = 23$ and 25 have as their symbols (0^{23}S) and (0^{23}10S), respectively. Note that all three symbols are required, since two periodic windows may differ not by the number of spikes per burst, but by the characteristics of spikes themselves. For instance, another $n = 23$ window was observed at $z_0 = 3.24$, which is of the type (0^{20}100S), different from the previous one. Besides, periodic windows may have several different bursts per period. We record here three such examples: (1) at $z_0 = 3.39814$, three bursts per period ($n = 19,19,20$), symbolic name = $(0^{17}10S)^2(0^{17}100S)$; (2) at $z_0 = 3.33945$, two bursts per period ($n = 20,21$), symbolic name = $(0^{18}10S)(0^{18}100S)$; and (3) at $z_0 = 3.339$, four bursts per period ($n = 20,20,20,21$), symbolic name = $(10^{18}10S)^3(0^{18}100S)$.

To conclude, chaotic bursting, as well as complex bifurcation sequences of periodic bursting, can be described and classified using a symbolic dynamics with three alphabets. They are however important only in a relatively small range of z_0 values near the onset point $(z_0)_{\text{II-III}}$ of bursting. This is explained by the fact that $|\Lambda_u|$ of the basic cycle becomes rapidly very large.

On the other hand, for z_0 away from the critical zone, say $z_0 > 3.2$, no chaos has been observed, and a simple sequence of periodic bursting is dominant (with $n = 21, \ldots, 7,6,5$ observed as z_0 is increased from 3.25 to 5.1). This *regular* sequence is not related to a homoclinic tangency to Ω. Rather, as z_0 is increased beyond 3.2, the reinjection is closer to Ω (compare fig. 2b with fig. 2d). This means that less iterations on the Poincaré map are needed for the reinjection, and the integer k in the definition of T_1 is reduced for increasing z_0. In this way the number of spikes per burst can decrease gradually with increasing z_0. Therefore, transitions between $n+1$ to n spikes in this sequence may even by continuous without a bifurcation [29]. The transition usually occurs as $(0^{n+1}) \rightarrow (0^{n-1}10) \rightarrow (0^n)$.

Comparing figs. 2a, b with 2c, d, we also note that for larger z_0 the orbit spends more time on the lower steady state branch of the fast subsystem, so that the silent phases are prolonged. In that region of the phase space the flow is virtually compressed onto an one-dimensional curve. This can already be seen in fig. 2d: orbits which are separate when escaping from the spiking region become visually indistinguishable at the end of the silent phase. For large z_0, during the prolonged silent phase the flow may be compressed practically onto the 1D curve, so that chaos is effectively eliminated.

2.6. *Crisis of the chaotic continuous spiking state*

We shall end with a characterization of the transition which takes place at $z_0 = (z_0)_{\text{II-III}}$. According to our hypothesis, the chaotic continuous spiking state Ω is destabilized at the critical point, when it merges with the invariant manifold $W_s(p) \times W_u'(p)$ of the equilibrium state p. In terms of the Poincaré section, since the invariant state Ω is confined on a quasi-one dimensional curve (fig. 3) which is near the unstable manifold of the fixed point of the map, we may surmise a more specific hypothesis: *the criticality occurs when the unstable manifold of a periodic orbit in Ω* merges with $W_s(p) \times W_u'(p)$.

This conjecture can be tested by considering how the mean escape rate γ of the chaotic state behaves near $(z_0)_{\text{II-III}}$. As we summarized in the introduction, γ is the order parameter of this critical phenomenon, which is positive for $z_0 > (z_0)_{\text{II-III}}$ and vanishes for $z_0 \leq (z_0)_{\text{II-III}}$. Our situation is similar to a type of *crisis* studied in [10], which is induced by a heteroclinic tangency between the unstable manifold of an unstable periodic orbit in a chaotic state Ω, and the stable manifold of another periodic orbit *outside* Ω. In that case, the mean escape rate γ tends to zero as the crisis is approached, according to a power law, with the exponent α given by

$$\alpha = \tfrac{1}{2} + (\ln|\Lambda_u|)/(\ln|\Lambda_s|)\,, \tag{11}$$

where Λ_s and Λ_u are the stable and unstable eigenvalues, respectively, of the periodic orbit in Ω. In the strongly contracting limit, $|\Lambda_s| = 0$, we have $\alpha = \frac{1}{2}$.

We found that the derivation of expression (11) can be carried over without change to our case of the HR model, except that the stable manifold of the second periodic orbit is here replaced by $W_s(p) \times W_u'(p)$ of the equilibrium state p. Hence, with the strong contraction we predict that the transition from continuous spiking to bursting is characterized by the following power law:

$$\gamma \sim (z_0 - (z_0)_{\text{II-III}})^{1/2}\,, \tag{12}$$

as $(z_0)_{\text{II-III}}$ is approached from above.

We have undertaken a numerical test of eq. (12). We did not compute separately the Lyapunov exponent λ_u of the continuous spiking chaos and its Kolmogorov–Sinai entropy h_{KS}, in order to subtract $\gamma = \lambda_u - h_{\text{KS}}$. Instead, we followed [10] to estimate γ via its inverse $\tau = 1/\gamma$, which is the mean residence time in Ω. Our numerical result shown in fig. 5 agrees with the theoretical prediction eq. (12).

Note that if the equilibrium state p *was* very close to Ω, for z_0 near $(z_0)_{\text{II-III}}$, it would have to

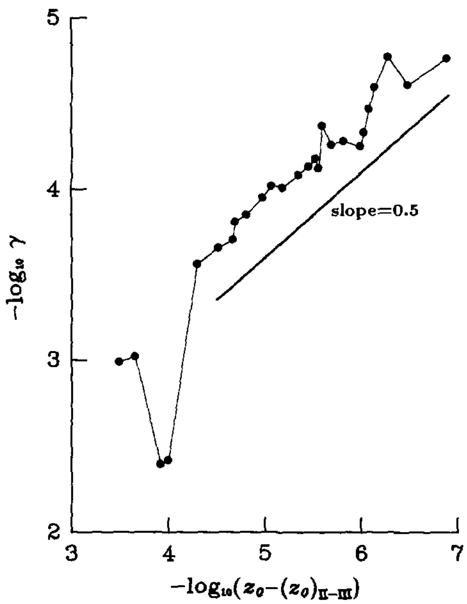

Fig. 5. Numerical estimation of the mean escape rate γ as z_0 approaches to the critical point $(z_0)_{II-III}$ from the bursting side. The solid circles are data points. At each fixed z_0, an orbit is integrated for a time of 6×10^5, which requires about 4×10^7 integration steps of variable size. The mean residence time of the orbit in Ω was evaluated, and its inverse yields an estimate of the γ. The data agree with the theoretical prediction eq. (12). The sudden drop at the beginning of the numerical curve corresponds to a periodic window ($n = 25$). Note that for the last few data points at the upper end, the integrated orbit contains only about ten bursts which become very long-lasting. Thus the mean is not accurately estimated due to the poor statistics.

affect the critical behavior, and eq. (12) would in fact need to be modified (cf. [10], subsection IV.B).

3. Concluding remarks

In this paper we discussed the genesis of bursting oscillations in a class of differential equations, exemplified by the Hindmarsh-Rose model. A specific mechanism, namely that of homoclinicity to a chaotic saddle, is proposed and tested favorably by numerical simulations. We also discussed the nature of the transition from continuous spiking to bursting, and obtained a quantitative characterization (eq. (12)) for its critical behavior.

A comparison is now in order between the bursting dynamics discussed here, and the Pomeau–Manneville intermittency [18]. The time evolution of this latter system also displays long regular phases of relative quiescence interrupted by bursts of large amplitude oscillations, and the underlying mechanism is also based on a reinjection principle. The critical intermittent systems should be compared with the bursting systems *at the crisis*: in both cases we have a codimension-one situation where a basic state becomes neutrally stable. To this basic state a reinjection mechanism is present. The difference between the two, however, is that for the intermittent dynamics the basic state is a periodic cycle; while for the bursting dynamics the basic state is a chaotic set. Consequently, *the quiescent phases* in the former case should be identified to the basic state, and the bursts to the reinjection loop. In the bursting case the opposite is true (fig. 6).

Away from the critical situation the basic state may acquire a hyperbolic structure, hence it becomes a saddle. Then, the reinjection mecha-

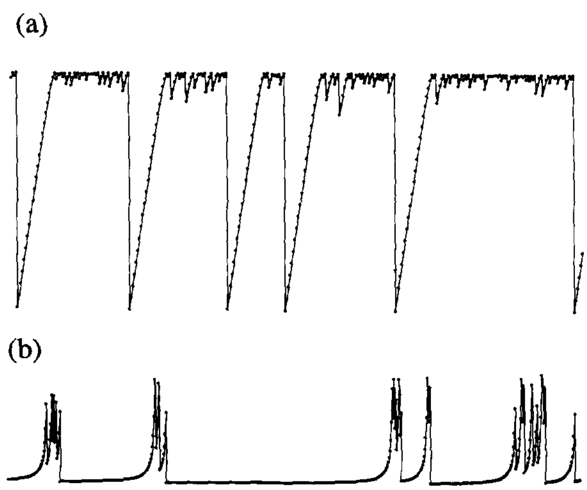

Fig. 6. Comparison of bursting dynamics near the criticality with the Pomeau–Manneville (PM) intermittent dynamics. (a) An iterative orbit of the 1D map $z_{n+1} = f(z_n;\ z_0 = 3.159)$ and (b) an orbit generated by the PM map $z_{n+1} = 0.01 + z_n + z_n^2$. Scales are arbitrary.

nism may create homoclinic orbits to this invariant saddle, and a critical situation of a different kind occurs when a homoclinicity is tangent. Here, it is the reinjection mapping, instead of the basic state, that is codimension one.

Therefore, the three types of complex multimodal oscillations (i.e. homoclinic systems, bursting and intermittency), which are of wide interest in various branches of natural sciences, may all be viewed as a reinjection mechanism to a certain invariant basic state.

Acknowledgements

It is a pleasure to thank J. Rinzel, D. Terman and A. Sherman for explaining to me their recent work, and for interesting discussions on the subject treated here. This work is partly supported by the Office of Naval Research under the contract No. N00014-90J-1194. The numerical simulations were carried out on the National Cancer Institute Advanced Scientific Computing Laboratory.

References

[1] J.C. Alexander and D.Y. Cai, J. Math. Biol. 29 (1991) 405.
[2] T.R. Chay and J. Keizer, Biophys. J. 42 (1983) 181.
[3] T.R. Chay and J. Rinzel, Biophys. J. 47 (1985) 357.
[4] O. Decroly and A. Goldbeter, J. Theor. Biol. 124 (1987) 219.
[5] E. Doedel, Cong. Num. 30 (1981) 265.
[6] J.-P. Eckmann and D. Ruelle, Rev. Mod. Phys. 57 (1985) 617.
[7] M.J. Feigenbaum, J. Stat. Phys. 19 (1978) 25.
[8] P. Gaspard and X.-J. Wang, J. Stat. Phys. 48 (1987) 151.
[9] N.K. Gavrilov and L.P. Šil'nikov, Math. USSR Sb. 17 (1972) 467, 19 (1973) 139.
[10] C. Grebogi, E. Ott and J.A. Yorke, Phys. Rev. A 36 (1987) 5365.
[11] J.L. Hindmarsh and R.M. Rose, Proc. R. Soc. Lond. B 221 (1984) 87.
[12] C. Kaas-Petersen, in: Chaos in Biological Systems, eds. H. Degn, A.V. Holden and L.F. Olsen (Plenum, New York, 1987) p. 183.
[13] T.-Y. Li and J.A. Yorke, Am. Math. Mon. 82 (1975) 985.
[14] C. Morris and H. Lecar, Biophys. J. 35 (1981) 193.
[15] S. Newhouse, Proc. AMS Symp. Pure Math. 14 (1970) 191.
[16] S. Newhouse, Topology 12 (1974) 9; Publ. Math. IHES 50 (1979) 101.
[17] I.M. Ovsyannikov and L.P. Šil'nikov, Math. USSR Sb. 58 (1987) 557.
[18] Y. Pomeau and P. Manneville, Commun. Math. Phys. 74 (1980) 189.
[19] J. Rinzel, in: Ordinary and Partial Differential Equations, eds. B.D. Sleemon and R.J. Jarvis (Springer, New York, 1985) p. 304.
[20] J. Rinzel, in: Proc. Int. Congress of Mathematicians, ed. A.M. Gleason (Am. Math. Soc., Providence, RI, 1987) p. 1578.
[21] J. Rinzel and Y.S. Lee, in: Nonlinear Oscillations in Biology and Chemistry, ed. H.G. Othmer (Springer, New York, 1986) p. 19.
[22] J. Rinzel and G.B. Ermentrout, in: Methods in Neuronal Modeling, From Synapses to Networks, eds. C. Koch and I. Segev (MIT Press, Boston, 1989) p. 135.
[23] C. Robinson, Commun. Math. Phys. 90 (1983) 433.
[24] A.I. Selverston and M. Moulin, Ann. Rev. Physiol. 47 (1985) 29.
[25] L.P. Šil'nikov, Soviet Math. Dokl. 6 (1965) 163; Math. USSR Sb. 10 (1970) 91.
[26] L.P. Šil'nikov, Soviet Math. Dokl. 9 (1968) 624.
[27] M. Steriade, E.G. Jones and R.R. Llinás, Thalamic Oscillations and Signaling (Wiley, New York, 1990).
[28] L. Tedeschini-Lalli and J.A. Yorke, Commun. Math. Phys. 106 (1986) 635.
[29] D. Terman, SIAM J. Appl. Math. 51 (1991) 1418.
[30] D. Terman, The transition from bursting to continuous spiking in excitable membrane models, preprint, Ohio State University at Columbus (1991).
[31] S.J. van Strien, Lecture Notes in Mathematics, Vol. 898 (Springer, Berlin, 1981) p. 316.
[32] X.-J. Wang, Commun. Math. Phys. 131 (1990) 317.